Physics of one-dimensional hybrids based on carbon nanotubes

Gao, Jia

Chapter 4

Effectiveness of sorting single-walled carbon nanotubes by diameter using polyfluorene derivatives

Semiconducting single-walled carbon nanotubes (SWNTs) sorted by conjugated polymers are of great interest for electronic and optoelectronic applications. In this chapter we demonstrate by optical methods that the selectivity of conjugated polymers for semiconducting SWNTs is influenced by the structure of their side-chains and/or the molecular weight of the macromolecules, and that side chain functionalities determine the solubility in different dispersion media. Moreover, high resolution time-resolved photoluminescence measurements provide evidence of energy transfer from tubes with larger band gaps towards those with smaller band gaps coexisting in SWNT bundles.[*]

4.1 Introduction

Because of the strong tendency of carbon nanotubes to aggregate and to form bundles, the first few studies on the optical properties of SWNTs had limited success in explaining the photophysics of these one-dimensional objects. SWNTs are hollow cylinders composed only of carbon atoms that have remained at the forefront of nanotechnology research for the last two decades. [1–3] Since the first result of band gap photoluminescence from SWNTs dispersed with sodium dodecyl sulfonate (SDS) in aqueous solution was reported, [4] many molecules and macromolecules, including sodium dodecylbenzene sulfonate (SDBS), [5] sodium cholate, sodium deoxycholate, [6, 7] and single-stranded DNA, [8] have been used for the same purpose. Other methods for selective separation of SWNTs include electrophoresis, chromatography, and density gradient ultracentrifugation. [9–11] Recently, π-conjugated polymers have proven to be very effective in solubilizing specific SWNTs. Among these polymers, polyfluorene homo- and co-polymers show unique selectivity for a narrow distribution of semiconducting species when dissolved in organic solvents. [12] The photophysical properties of such polymer/SWNT hybrids were explored from many aspects at later stage. Recently, Hwang et al. reported on the polymer structure and solvent effects on the selectivity of SWNT dispersion. [13] Other authors have studied the interaction between the wrapped polymer chains and SWNTs. [14, 15] However, the mechanism of the unique interaction of poly(9,9-di-n-octylfluorenyl-2,7-diyl) (PFO) and its copolymer with SWNTs is still a matter for investigation. The fact that many of the co-polymers used have had different backbone structures compared to that of PFO serves to complicate relative studies. Moreover, water-soluble polyfluorene derivatives may also evidence selectivity for SWNT dispersion, which might be helpful for the application of SWNTs in biology. However, up to now no such studies have been reported. It would therefore be highly desirable to gain a deeper understanding of the role of the backbone and side-chain structures on the selectivity for specific SWNT.

In our work, we studied the photophysics of SWNT dispersion with amine-functionalized polyfluorene (poly(9,9- di-(N,N-dimethylaminopropylfluorenyl-2,7-diyl) (PFDMA)) and its ammonium salts [(N,N,N-trimethylammonium)-propyl]-2,7-fluorene dibromide) (PFAB) in different media. We found that the selectivity for SWNTs of PFDMA in toluene is different than that of PFO.

New absorption and photoluminescence (PL) peaks appear in PFDMA/SWNTs spectra, indicating the presence of a larger number of nanotube species. SWNT dispersions with PFAB in D_2O contain similar species to the PFDMA-based

dispersion in toluene, with a universal shift of the PL peaks due to the change of effective dielectric constant of the medium. Photoluminescence decays of dispersed SWNTs indicate that the intrinsic lifetime of the 'bright' exciton in SWNTs is in the range of 28–40 ps. More importantly, the PL lifetimes of carbon nanotubes with different band-gaps show diverse lifetimes, indicating exciton energy transfer in residual SWNT bundles that leads to PL quenching of nanotubes with larger energy band gap compared to those with smaller band gap.

4.2 Results and discussion

The absorption and photoluminescence spectra of diluted solutions of PFAB, PFDMA, and PFO are shown in Figure 4.1. All samples showed a broad absorption ranging from 350 nm to 400 nm with absorption maxima at 393 (PFAB), 379 (PFDMA), and 386 nm (PFO), respectively. In the case of PFO/toluene solution, the main peak with no vibronic structure is assigned to the α-phase, and the resolved shoulder at 436 nm is due to the β-phase, as reported in previously. [16] PFDMA has short N,N-dimethylamino side chains at the 9 position of the fluorene unit and shows a better solubility than PFO, which exhibits linear octyl chains. This is evidenced both by the faster dissolution and by the lack of shoulder in the absorption spectrum of PFDMA. The main absorption peak of PFAB is red-shifted by 14 nm compared to that of PFDMA. This spectral difference may be due to the charged side-chains or to the larger dielectric constant of the environment (ϵ_{D_2O}=78 vs $\epsilon_{toluene}$=2.4). The steady-state PL spectra of all the samples display two sharp bands and a weak shoulder in the range of 400-500 nm (Figure 4.1).
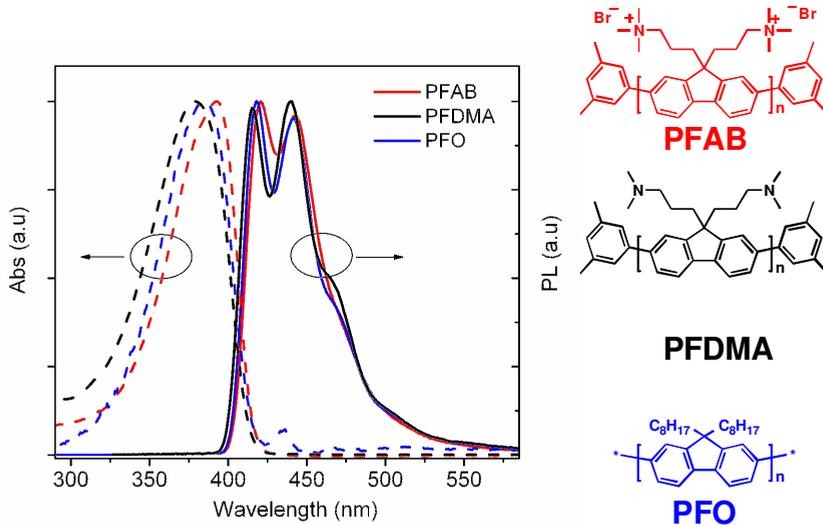
Figure 4.1 Absorption (dashed lines) and photoluminescence (solid lines) spectra of PFO (blue lines), PFDMA (black lines) toluene solutions and PFAB (red lines) D$_2$O solution. The spectra are normalized at their maximum intensity. The chemical structures of the polymers are shown at the right side of the figure.

The absorption and photoluminescence spectra of HiPCO SWNTs (H-NT) dispersed with the three polymers at the weight ratio of 1 to 5 are shown in Figure 4.2. Both absorption and PL spectra reveal a large difference in the capability of PFDMA and PFAB to disperse SWNTs selectively in respect to PFO. It should be mentioned that not only the structures of the polymer but also the weight ratio of the polymer and SWNTs might influence the selectivity for specific carbon nanotube species, as was recently reported. [17] However, in our study we found that the selectivity of the three polymers remains constant when the weight ratio of SWNTs to polymer is in the range between 1:1 and 1:10. It is logical to conclude that the different selectivity is caused by the polymer structure and not by other effects.

In the absorption spectrum of the PFO sorted SWNTs (Figure 4.2(c)), the peaks at wavelength higher than 900 nm are the E$_{11}$ transitions of 5 different SWNT species corresponding to (7,5), (7,6), (8,6), (8,7), and (9,7), according to the empirical kataura plot. [18, 19]

PFAB proved to be effective for SWNT dispersion in D$_2$O (Figure 4.2(a)). However, in this case ultracentrifugation was necessary for the separation of the sorted SWNTs and bigger bundles by buoyant forces.

This is understandable by simply taking into account the density of the two solvents, 1.1 g/cm^3 for D$_2$O and 0.9 g/cm^3 for toluene. The sonicated SWNT dispersion with PFAB was ultra-centrifuged at 65k rpm for 2 h, as was the SWNTs

dispersion in standard aqueous surfactants. [4] By using optical measurements on the dispersion, we found that PFAB in water shows similar selectivity for SWNTs as PFDMA in toluene (see Figure 4.2(a) and 4.2(b)). Moreover, the selectivity shown by PFAB in D_2O was not dissimilar to that observed for SDBS-based dispersions.

The absorption spectra of SWNT dispersions of PFAB and PFDMA (Figure 4.2(a), 4.2(b)) show higher background intensity and less-resolved features than the PFO-based SWNT dispersion (Figure 4.2(c)), indicating the presence of more residual bundles in solution. Moreover, optical transitions from metallic tubes in the range of 500-600 nm were observed exclusively in the dispersions with PFAB and PFDMA (Figure 4.2(a) and 4.2(b)). The concentration of dispersed SWNTs was calculated by using the value for absorption cross section, as reported recently. [20] The result is 0.5 µg/mL for PFO/toluene dispersion, 0.8 µg/mL for PFDMA/toluene dispersion, and 1.2 µg/mL for PFAB/D_2O dispersion, respectively. In general, although the amino-substituted polymers yield higher total amounts of dispersed nanotubes, the selectivity of these polymers for semiconducting carbon nanotubes is lower than that of PFO.

Steady-state photoluminescence measurements were used to probe individual SWNTs and/or small semiconducting bundles in the three dispersions (Figure 4.2(d)-(f)). The PL spectrum of the PFO dispersed SWNTs, depicted in Figure 4.2(f), shows the highest PL intensity and the least full width at half maximum (FWHM) of the single peaks. Lower PL intensity and broader peaks were found for PFDMA/toluene and PFAB/D_2O dispersions (Figure 4.2(d) and 4.2(f)). This is a further indication of the presence of bundles in the solution and is therefore in accordance with the results of the absorption measurements.

In the case of PFAB/D_2O dispersion, the PL spectra of the SWNTs (Figure 4.2(d)) are red-shifted by about 8 nm compared to those dispersed with PFDMA and PFO in toluene (Figure 4.2(e) and 4.2(f)). Such a shift has been explained previously as due to the dielectric constant of the solvent. [21] In order to rule out any effects due to the counter ions present in the side-chain of PFAB, we studied the SWNT dispersion in aqueous solution using a polymer with the same structure but with a different counter ion, namely poly(9,9-bis{3'-[(N,N,N-trimethylammonium}-propyl]-2,7-fluorene di-(methyl sulfonate)) (PFAS). Optical experiments showed identical results for dispersions with this polymer as for PFAB-wrapped SWNTs This comparison demonstrates that the counter ions of PFAB do not affect the capability of the polymer to wrap around SWNTs and leave the physical properties of the nanotubes unchanged.

Figure 4.2 Absorption and photoluminescence spectra of HiPCO SWNTs dispersion with different polymers and solvents. Absorption spectra of SWNTs dispersed with, (a) PFAB/D_2O, (b) PFDMA/tol, (c) PFO/tol. PL spectra of SWNTs dispersed with, (d) PFAB/D_2O, (e) PFDMA/tol, (f) PFO/tol.

It is important to note that CoMoCAT SWNTs (C-NT) sorting was also obtained and showed analogous behavior to the HiPCO tubes (Figure. 4.3).
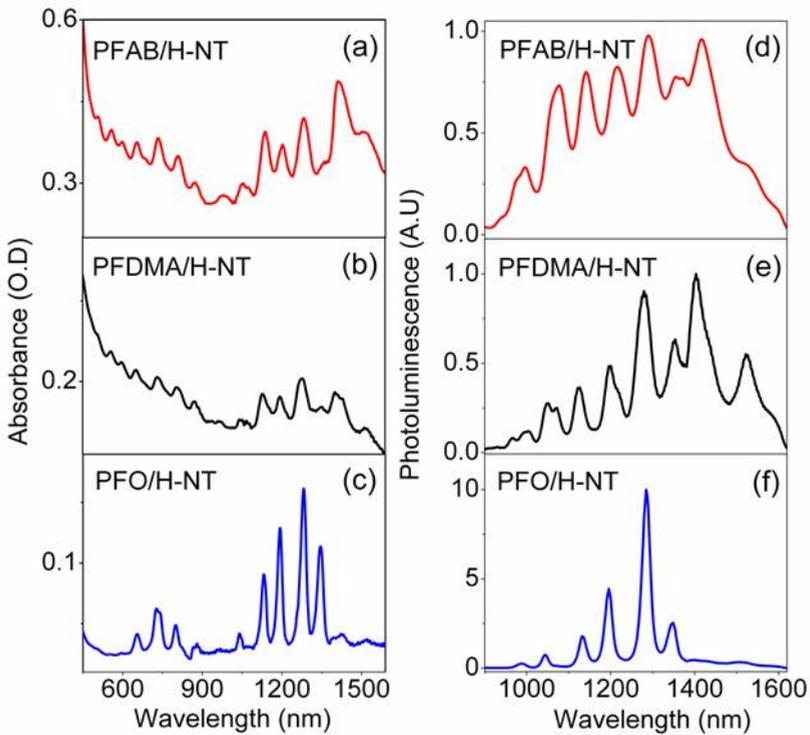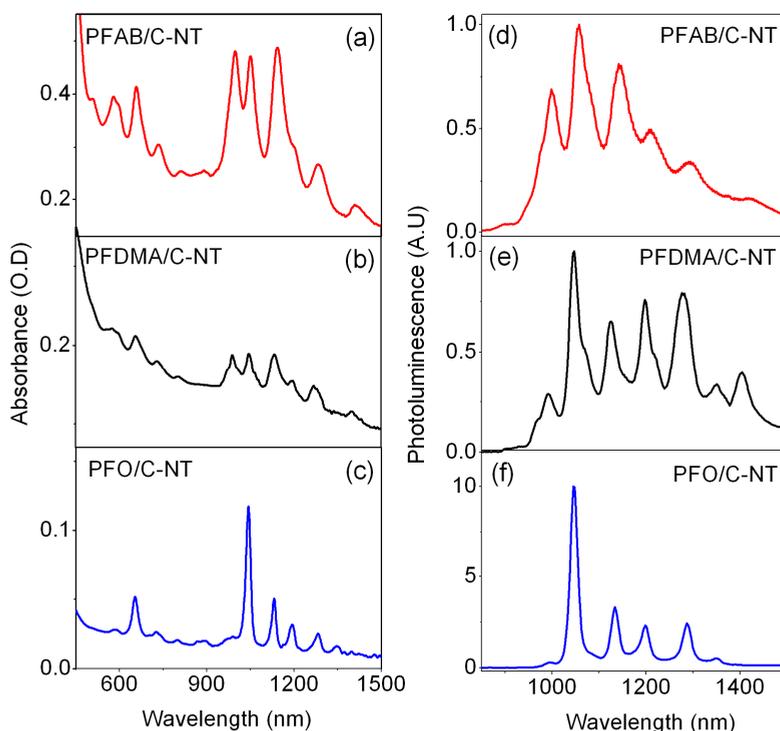
Figure 4.3 Absorption and photoluminescence spectra of Comocat SWNTs dispersion with different polymers and solvents. Absorption spectra of SWNTs dispersed with, (a) PFAB/D$_2$O, (b) PFDMA/tol, (c) PFO/tol. PL spectra of SWNTs dispersed with, (d) PFAB/D$_2$O, (e) PFDMA/tol, (f) PFO/tol.

We conjecture that the different selectivity for SWNTs of PFDMA and PFAB with respect to PFO is due to their different side chain structures and molecular weights, which leads to dissimilar interactions of the polymers with the nanotube side-walls. It is necessary to stress that in addition to the difference in the chemical nature of the side chain, the molecular weight of PFDMA (and PFAB) synthesized via Pd(0)-catalyzed Suzuki coupling is much lower than that of PFO, which may also influence the interaction of the macromolecule with the carbon nanotube's walls. On the other hand, the well-known affinity of amino groups to carbon nanotubes could influence the recognition capability of the PFDMA as well. [22] Further studies that take these possibilities into account are currently underway.

The dynamics of the excitons in SWNTs was studied with the aid of a high resolution streak camera (~3 ps), sensitive in the near infrared range. Figure 4.4 shows the spectrally and time-resolved PL of the three dispersed SWNT samples (Figure 4.4(a)-(c)) and the PL decays in different spectral ranges corresponding to

the emission of (6,5) and (7,5) tubes (Figure 4.4(d)-(f)). The PL decays of both (6,5) and (7,5) tubes can be fitted with a bi-exponential function, where τ_1 and τ_2 represent the short and long time constants, respectively. The response of the instrument is also included. The first decay component, τ_1, is in the range of 4-14 ps and varies depending on the polymer used for the dispersion. For the PFO/toluene system, the (7,5) tube has $\tau_1 \sim 14$ ps (Figure 4.4(f)), while the decay of the (6,5) tubes is not considered here, due to the negligible PL intensity. For PFAB-wrapped tubes, the first decay component of both tubes is of 5 ps and 6 ps, respectively (Figure 4.4(d)), where τ_1 is 4 ps for (6,5) tubes and 8 ps for (7,5) tubes for PFDMA-based hybrids (Figure 3(e)).

All the dispersions were excited at 760 nm, which is a non-resonant condition for (6,5) and (7,5) tubes. Excited electrons relax rapidly into the lowest energy level of the conduction band and excitons formed due to the large binding energy [a few hundred millielectronvolts] in semiconducting species. Photoluminescence can only be observed from 'bright' excitons. The first decay component in the range of 4-14 ps is attributed to the non-radiative loss of 'bright' exciton towards intrinsic 'dark' excitonic states, wall defects, and by inter-tube interaction in residual bundles. [23-26] Conversely to the first decay time, both nanotube species in all the dispersions show a long decay component τ_2 in the range of 28-40 ps, which we attribute to the intrinsic lifetime of this SWNT species. This is consistent with previous reports regarding small diameter tubes. [27] It is important to note that the wrapping of the polymer around the SWNTs modifies locally the dielectric constant, this is especially important when using media with dielectric constant very different from the media of the polymer ($\varepsilon \sim 2$-2.5).

The variation of the PL lifetime of the first decay component in the polymer dispersed carbon nanotubes is in agreement with an energy transfer between species of different band-gap, which appears to commonly occur in SWNT bundles. [28] This interaction is one of the most elusive effects in carbon nanotubes photophysics, in that the investigation of these effects is strongly limited by the quality and control of the nanotubes separation. [29] Up to now, very few studies on energy transfer in SWNT aggregates based on steady-state measurements such as high-resolution optical microscopy and photoluminescence excitation spectroscopy have been reported. [30-35] It is known, however, that precise information of the energy transfer can be obtained only with time-resolved spectroscopy. [36]

Among all the species of nanotubes in the dispersions, (7,5) and (6,5) tubes have larger energy band gaps, which make their emission properties sensitive to inter-tube energy transfer when they are in bundles. As we have demonstrated above, SWNT dispersions with PFO/toluene solution contain almost no SWNT bundles. This is further evidenced by the fact that the decay time is the longest of all three dispersions ((7,5) tube (τ_1=14 ps, τ_2=38 ps). The dispersions with PFDMA and

with PFAB contain small bundles, and the PL decay of the (7,5) tube are τ_1=8 ps, τ_2=35 ps and τ_1=6 ps, τ_2=30 ps, respectively. Moreover, in the PFDMA/toluene dispersion the fluorescence decay of (6,5) tubes (larger band gap tube) is faster (4 ps) than that of (7,5) tubes (8 ps), suggesting an efficient interaction between the larger band-gap nanotube (6.5) and the surrounding smaller band gap nanotubes ((7.5) and smaller band gap tubes).

Very recently, Lüer et al [37] reported ultrafast (less than 10 fs) energy transfer in small SWNT bundles by transient absorption spectroscopy. Although our measurements have inferior time resolution (3 ps), the results obtained are in agreement with this recent report.

Finally, our study demonstrates that time-resolved spectroscopy is the better tool in order to evaluate the quality and the separation of semiconducting SWNT dispersion because it allows for the observation of inter-tube energy transfer in small bundles.
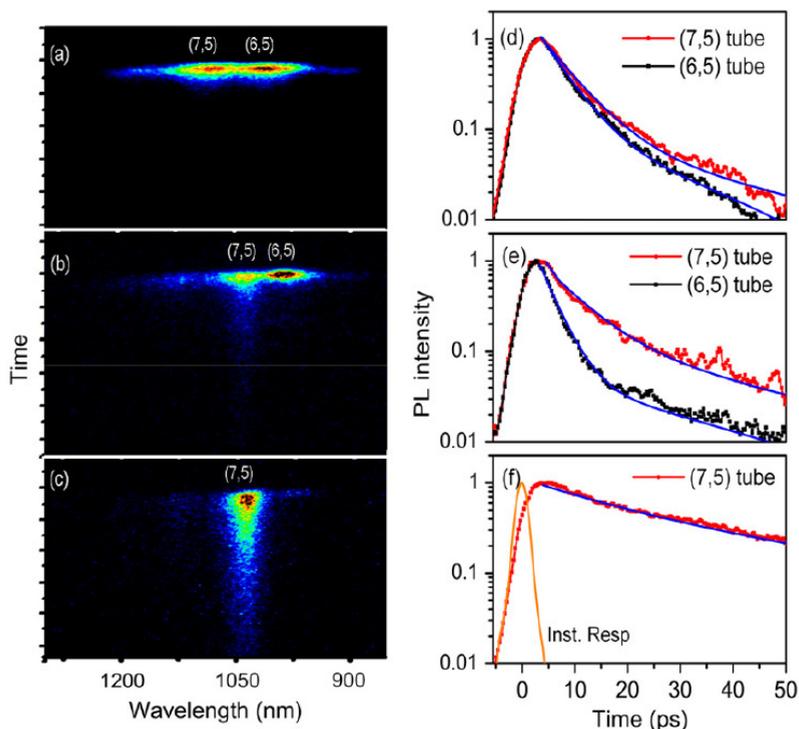
Figure 4.4 Intensity matrix of spectrally and time resolved PL of nanotubes sorted with, (a) PFAB/D$_2$O, (b) PFDMA/tol, (c) PFO/tol. PL decays (6,5) and (7,5) SWNTs dispersed with, (d) PFAB/D$_2$O, (e) PFDMA/tol, (f) PFO/tol. The blue lines are the fitting curves with two exponential components. The intensity is normalized at t=0. The samples were excited at 760 nm.

4.3 Conclusions

We have presented the photophysics of semiconducting SWNTs sorted by wrapping with different polyfluorene derivatives. The side chain functionalities were used for achieving SWNT dispersion in different solvents. We demonstrated that SWNT dispersions are influenced by the molecular weight and the structure of side-chains of the polymer. The intrinsic lifetime of the small diameter SWNTs measured in ensemble was found to be in the range of 28-40 ps. Moreover, we provided evidence of energy transfer from tubes with larger band gap to those with smaller band gaps occurring in SWNT bundles. These results confirm the results of poor selectivity found in the steady state experiments for the PFAB and PFDMA and further demonstrate that time-resolved PL is a very efficient analytical tool to estimate the degree of individual isolation of semiconducting SWNTs in solution.

4.4 Experimental details

Polymer synthesis

Poly(9,9-di-(N,N-dimethylaminopropylfluorenyl-2,7-diyl) (PFDMA) was prepared via Pd(0)-catalyzed Suzuki coupling of dibromo- and diboronic acid pinacol ester-fluorene monomers. This polymer was quarternized by the addition of methyl halide to form PFAB.
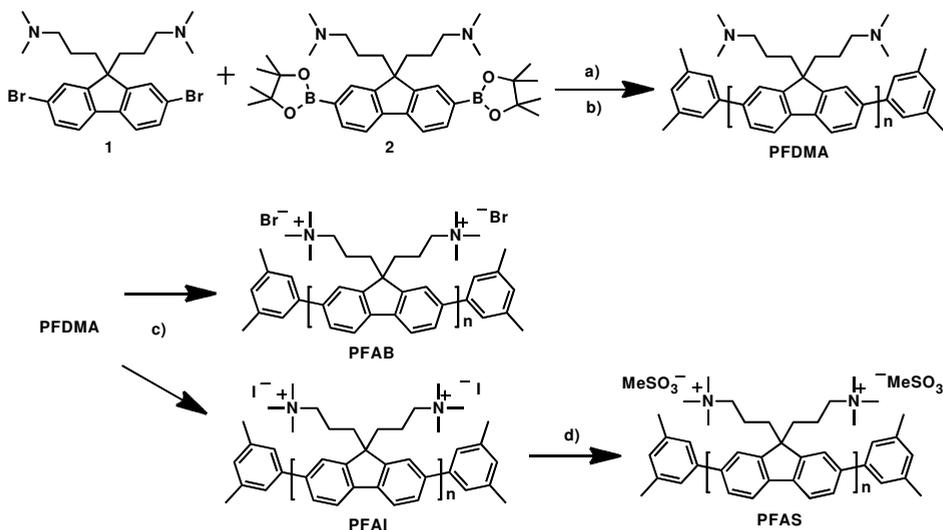
Scheme S1 Preparation of water-soluble polymers PFAB and PFAS. (a) Tetrabutylammonium bromide (TBAB), tetrakis(triphenylphosphine)palladium (0) (Pd(PPh$_3$)$_4$,), KOH, toluene, reflux, 16 h. (b) 1-Bromo-3,5-dimethylbenzene, Pd(PPh$_3$)$_4$, reflux, 2 h. (c) CH$_3$Br (or CH$_3$I), THF, r.t., 16 h. (d) AgMeSO$_3$, H$_2$O, 16 h.

PFDMA was prepared according to a previously reported synthetic procedure with slight modifications for end-capping. Both the dimethylaminopropyl groups at the 9-position of PFDMA were quarternized by adding methyl bromide (Scheme S1a) or methyl iodide (Scheme S1b). Synthesis of PFDMA, In a two-neck round-bottomed flask purged with nitrogen, 2,7-dibromo-9,9'-bis(3'-(N,N-dimethylamino)propyl)fluorene (1) (998 mg, 2.00 mmol), 2,7-bis(4,4,5,5-tetramethyl-1,3,2-dioxaborolane)-bis(3'-(N,N-dimethylamino)propyl)fluorene (2) (1.205 mg, 2.05 mmol), toluene (25 mL), KOH solution (8 mL, 20 %), and 30 mg of TBAB (ca. 0.1 mmol), and Pd(PPh$_3$)$_4$ (25 mg, 0.025 mmol) were mixed and

refluxed for 16 h. To the reaction mixture, 1-bromo-3,5-dimethylbenzene (18 mg, 0.1 mmol), and Pd(PPh$_3$)$_4$ (3 mg, 0.003 mmol) were added and refluxed for another 2 h. NaCN dissolved in 10 mL of water was added to the mixture and stirred for 18 h, centrifuged, and then the aqueous layer was removed. After removal of solvent, the polymer was dissolved in THF and then precipitated in a 20-fold volume excess of water. The precipitate was washed with water and dried in a desiccator on KOH to yield 580 mg (43%).

1H NMR (400 MHz, CDCl$_3$), δ = 7.85−7.80 (d, 22H), 7.71−7.66 (m, 44H), 7.49−7.45 (6H), 2.12−2.03 (br m, 240H), 1.03-0.92 (s, 44H).

The molecular weight determined by 1H NMR is 4.6 kDa / mol and by GPC, M_n = 2,117 and M_w = 2,704 with the polydispersity index 1.27 upon polystyrene reference. For PFO from Sigma-Adrich, M_n = 15834.

Synthesis of PFAB, PFDMA (1.0 g) was dissolved in THF and 1 mL of MeBr (or MeI for the preparation of PFAI) was added and further stirred at room temperature for 16 h. The mixture was additionally refluxed for 1 h. The solid was filtered and washed with ether to yield a yellow solid (1.13 g, 77%).

Synthesis of PFAS, To a solution of PFAI (500 mg) in warm water (40 mL), Ag-methylsulfate (2.0 equivalent) was added, a solid of AgI was formed immediately, and stirred for 16 h. The reaction mixture was centrifuged and the supernatant was decanted. After removal of water from the mixture by rotary-evaporator, acetone was added to precipitate the product, filtered, and subsequently washed with to yield a yellow solid (800 mg).

The molecular weight of PFDMA was found to be almost one order of magnitude lower than that of PFO, which was purchased from Sigma–Aldrich (The Netherlands) and used as received.

SWNT dispersion preparation

Two kinds of carbon nanotubes, CoMoCAT SWNT (C-NT) from Southwest Nanotech and HiPCO SWNT (H-NT) from Carbon Nanotechnologies, were used as received. The CoMoCAT SWNTs were characterized by a narrower diameter distribution in respect to the HiPCO SWNT (H-NT). For the preparation of SWNT dispersions, dry nanotubes were added to 6 mL of polymer solution in a weight ratio of 1mg SWNT to 1–10 mg polymer, and the mixture was sonicated for 4 h in a tabletop ultrasonic bath (VWR, The Netherlands). After sonication, the crude dispersion was centrifuged at 5k rpm for 20 min, and the aqueous dispersion was ultracentrifuged at 65k rpm for 2 h. The supernatant was then removed for further measurements.

Optical spectroscopy

Absorption spectra were recorded with a Perkin-Elmer UV/Vis/NIR spectrophotometer (Lambda 900). Steady-state and time-resolved photoluminescence measurements were performed, exciting the solutions at 760 or 380 nm by a 150 fs pulsed Kerr mode locked Ti-sapphire laser. The steady-state PL of SWNTs and polymers were measured with InGaAs and Si-CCD detectors, respectively. The time-resolved PL of the dispersion was recorded by a Hamamatsu streak camera working in synchroscan mode, with photocathode sensitive in the near infrared spectral range. All the measurements were performed at room temperature, and the spectra were calibrated for the instrumental response.

References

[1] S. Iijima, T. Ichihashi, *Nature* **1993**, *363*, 603-605.

[2] M. Bockrath M, D. H. Cobden, P. L. Mceuen, N. G. Chopra, A. Zettl, A. Thess, R. E. Smally, *Science* **1997**, *275*, 1922-1925.

[3] R. Martel R, T. Schmidt, H. R. Shea, T. Hertel, P. Avouris, *Appl. Phys. Lett.* **1998**, *73*, 2447-2449.

[4] M. J. O'Connell, S. M. Bachilo, C. B. Huffman, V. C. Moore, M. S. Strano, E. H. Haroz, K. L. Rialon, P. J. Boul, W. H. Noon, C.Kittrell, J. Ma, R. H. Hauge, R. B. Weisman, R. E. Smalley, *Science* **2002**, *297*, 593-596.

[5] M. F. Islam, E. Rojas, D. M. Bergey, A. T. Johnson, A. G. Yodh, *Nano Lett* **2003**, *3*, 269-273.

[6] W. Wenseleers, I. I. Vlasov, E. Goovaerts, E. D. Obraztsova, A. S. Lobach, A. Boouwen, *Adv. Funct. Mater.* **2004**, *14*, 1105-1112.

[7] Okazaki T, Saito T, Matsuura K, Ohshima S,Yumura M, Iijima S. *Nano. Lett* **2005**, *5*, 2618-2623.

[8] M. Zheng, A. Jagota, E. D. Semke, B. A. Diner, R. S. Mclean, S. R. Lustig, R. E. Richardson, N. G. Tassi, *Nat. Mater* **2003**, *2*, 338-342.

[9] D. A. Heller, R. M. Mayrhofer, S. Baik, Y. V. Grinkova, M. L. Usrey, M. S. Strano. *J. Am. Chem. Soc.* **2004**, *126*, 14567-14573.

[10] L. Zhang, S. Zaric, X. Tu, X. Wang, W. Zhao, H. Dai, *J. Am. Chem. Soc* **2008**, *130*, 2686-2691.

[11] M. C. Hersam, *Nat. Nanotechnol* **2008**, *3*, 387-394.

[12] F. Chen, B. Wang, Y. Chen, L. J. Li, *Nano Lett* **2007**, *7*, 3013-3017.

[13] J. Y. Hwang, A. Nish, J. Doig, S. Douven, C. W. Chen, L. C. Chen, R. J. Nicholas, *J. Am. Chem. Soc* **2008**, *130*, 3543-3553.

[14] J. Gao, M. A. Loi, *Eur. Phys. J. B* **2010**, *75*, 121-126.

[15] F. Chen, W. Zhang, M. Jia, L. Wei, X. F. Fan, J. L. Kuo, Y. Chen, M. B. Chan-Park, A. Xia, L. -J. Li, *J. Phys. Chem. C* **2009**, *113*, 14946-14952.

[16] M. Grell, D. D. C. Bradley, X. Long, T. Chamberlain, M. Inbasekaran, E. P. Woo, M. Soliman, *Acta Polym* **1998**, *49*, 439-444.

[17] N. Sturzl, F. Hennrich, S. Lebedkin, M. M. Kappes, *J. Phys. Chem. C* **2009**, *113*, 14628-14632.

[18] A. Nish, J. Y. Hwang, J. Doig, R. J. Nicholas, *Nat. Nanotechnol* **2007**, *2*, 640-646.

[19] H. Kataura, Y. Kumazawa, Y. Maniwa, I. Umezu, S. Suzuki, Y. Ohtsuka, Y. Achiba, *Synth. Met* **1999**, *103*, 2555-2558.

[20] S. Berciaud, L. Cognet, B. Lounis, *Phys. Rev. Lett* **2008**, *101*, 077402

[21] Y. Ohno, S. Iwasaki, Y. Murakami, S. Kishimoto, S. Maruyama, T. Mizutani, *Phys. Status. Solidi. B* **2007**, *244*, 4002-4005.

[22] M. C. Lemieux, M. Roberts, S. Barman, Y. W. Jin, J. M. Kim, Z. Bao, *Science* **2008**, *321*, 101-104.

[23] M. Jones, W. K. Metzger, T. J. McDonald, C. Engtrakul, R. G. Ellingson, G.

Rumbles G, M. J. Heben, *Nano Lett* **2007**, *7*, 300-306.

[24] J. S. Lauret, C. Voisin, C. Cassabois, C. Delalande, R. H. Roussignol, O. Jost L. Capes, *Phys Rev Lett* **2003**, *90*, 057404.

[25] Z. Zhu, J. Crochet, M. C. Arnold, M. C. Hersam, H. Ulbricht, D. Resasco, T. Hertel, *J. Phys. Chem. C* **2007**, *111*, 3831-3835.

[26] S. Berger, C. Voisin, G. Cassabois, C. Delalande, P. Roussignol, *Nano Lett* **2007**, *7*, 398-402.

[27] H. Hirori, K. Matsuda, Y. Miyauchi, S. Maruyama, Y. Kanemitsu, *Phys. Rev. Lett* **2006**, *97*, 257401.

[28] Y. Homma, S. Chiashi, Y. Kobayashi, *Rep. Prog. Phys* **2009**, *72*, 066502.

[29] L. J. Carlson, T. D. Krauss, *Acc. Chem. Res* **2008**, *41*, 235-243.

[30] H. Qian, C. Georgi, N. Anderson, A. A. Green, M. C. Hersam, L. Novotny, A. Hartschuh, *Nano Lett* **2008**, *8*, 1363-1367.

[31] J. Lefebvre, P. Finnie, *J. Phys. Chem. C* **2009**, *113*, 7536-7540.

[32] O. N. Torrens, D. E. Milkie, M. Zheng, J. M. Kikkawa, *Nano Lett* **2006**, *12*, 2864-2867.

[33] T. Kato, R. Hatakeyama, *J. Am. Chem. Soc* **2008**, *130*, 8101-8107.

[34] P. H. Tan, A. G. Rozhin, T. Hasan, P. Hu, V. Scardaci, W. I. Milne, A. C. Ferrari, *Phys. Rev. Lett* **2007**, *99*, 137402.

[35] F. Chen, J. Ye, M. Y. Teo, Y. Zhao, L. P. Tan, Y. Chen, M. B. Chan-Park, L-Jong. Li *J. Phys. Chem. C* **2009**, *113*, 20061-20065.

[36] G. Bongiovanni, C. Botta, G. Di Silvestro, M. A. Loi, A. Mura, R. Tubino *Chem. Phys. Lett* **2001**, *345*, 386-394.

[37] L. Lüer, J. Crochet, T. Hertel, G. Cerullo, G. Lanzani, *ACS Nano* **2010**, *4*, 4265-4273.